# Thermoelectric Properties of $LaTe_y$

L.R. Danielson and M.N. Alexander

Thermo Electron Corporation

Waltham, Massachusetts 02254

C. Vining, R.A. Lockwood, and C. Wood

Jet Propulsion Laboratory, California Institute of Technology

Pasadena, California 91109

## ABSTRACT

Several lanthanum tellurides have been synthesized from the pure elements, hot pressed into test samples and measured. These samples have compositions $LaTe_y$, $1.33 \leq y \leq 1.48$, and all exhibit the thorium phosphide structure. The use of low-oxygen tellurium in the synthesis significantly reduced the oxygen in the final product compared to lanthanide telluride samples previously prepared at Thermo Electron. Electrical resistivities increase with both temperature and y, and Seebeck coefficients are negative and increase in magnitude monotonically with temperature and y. As y

increases, the degree of degeneracy decreases and the effective mass computed from the Seebeck coefficient becomes temperature dependent.

## I. INTRODUCTION

The lanthanum tellurides have recently attracted attention as high temperature n-type thermoelectric materials.[1] The compositions $LaTe_y$, $1.33 \leq y \leq 1.50$, are of particular interest since they form a continuous series of solid solutions having the $Th_3P_4$ structure and exhibit a wide range of carrier concentration. Based on results from $CeS_y$ and $LaS_y$,[3,4] $1.33 \leq y \leq 1.50$, which also have the $Th_3P_4$ structure, the density of conduction electrons should vary from zero to $4.5 \times 10^{21}/cm^3$ according to

$$n = \frac{4}{a^3}\left[\frac{3}{y} - 2\right] \quad 1.33 \leq y \leq 1.50 \qquad \text{Eq. 1}$$

where "a" is the $Th_3P_4$ lattice constant. The thermoelectric properties (Seebeck coefficients, electrical resistivities, and thermal conductivities) thus depend on the value of y.

Previous investigations of $LaTe_y$ as thermoelectric materials [1] indicated thermoelectric figures-of-merit near $1 \times 10^{-3}/^oC$ for some samples; however, the starting materials and/or processing techniques introduced small amounts (~5%) of $La_2O_2Te$ into these samples as a second phase. In addition, the lanthanum telluride compositions only

varied from $LaTe_{1.40}$ to $LaTe_{1.45}$. The objective of the current work was to prepare under well-controlled conditions single phase lanthanum telluride samples spanning nearly the whole range of solid solutions and to measure and analyze their thermoelectric properties.

## II. MATERIAL PREPARATION

Lanthanum was obtained in the form of ingots from Ames Laboratory (Ames, Iowa). Mass spectrometric and vacuum fusion analyses of the lanthanum indicated less than 0.13 at.% of both metallic and non-metallic impurities, of which 0.04 at.% was oxygen. Triple zone-refined tellurium (approximately 2 ppm by weight oxygen) was obtained as an ingot from Cabot, Inc. It was broken into large chunks in air and was crushed to -60 mesh in helium.

Processing (including weighing to 0.001 gm) and storage of the elemental constituents was performed in an argon-filled glove box having a moisture level less than 0.1 ppm by volume. In the glove box, lanthanum was slivered and mixed together with the tellurium into an outgassed quartz ampule. The loaded quartz ampules were sealed off under a pressure of $5 \times 10^{-6}$ Torr and transferred to resistance heated furnaces. The ampules were held at 220-250°C for several days to react the lanthanum and tellurium. The temperature was then increased

to 700°C over 2-3 days, and finally held at 700°C for approximately 20 hours to improve homogeneity.

The resulting powder was melted (1800°C for 30 minutes) in pressure-sealed tungsten crucibles, ground to -400 mesh in the argon filled glove box, loaded into a die and quickly transferred to a vacuum hot press. The powder was in contact only with outgassed graphite during the hot pressing. Samples were hot pressed at 1200°C and 7,500 psi for 1 hour. The samples were 1 to 1.5 cm long and 1.23 cm in diameter and possessed densities greater than 98.7% of the theoretical values.

X-ray diffraction analyses of both the powder after melting and the hot pressed samples showed a single phase $Th_3P_4$ structure. Lattice constants, shown in Figure 1, were determined for the ground powders after melting; the error bars represent the standard deviation of the y-intercept on Nelson-Riley graphs. The linear least squares fit to the data points shown in Figure 1 indicate a very slight decrease (0.05%) of the lattice constant as y varies from 1.33 to 1.48.

## III. THERMOELECTRIC MEASUREMENTS

Seebeck coefficients and electrical resistivities were measured from room temperature to 1000°C on an automated version of an

apparatus described previously.[5] Each Seebeck coefficient was calculated from a linear least-squares fit to 20 pairs of voltage and temperature differences. Correlation coefficients greater than 0.95 and zero-voltage temperature offsets of less than 2°C were required to accept each Seebeck coefficient point. Electrical resistivities were obtained by measuring the voltages across the niobium thermocouple leads for forward and backward currents of 100 mA through the sample.

Measurements of Seebeck coefficients (S), electrical resistivities ($\rho$), and power factors ($S^2/\rho$) are shown in Figures 2-5. The magnitudes of the n-type Seebeck coefficients for the $LaTe_y$ samples increase monotonically with y and with temperature. Electrical resistivities for $LaTe_{1.33}$ and $LaTe_{1.36}$ increase linearly with temperature, indicating degenerate itinerant conduction. For $LaTe_y$ with $y \leq 1.40$ the resistivities increase faster than linearly, indicating election mobilities decrease more rapidly than $T^{-1}$. No correlation of power factor with y is evident, except that the low power factor of $LaTe_{1.48}$ is expected because of its high resistivity. A maximum power factor near $15\mu\Omega/cm\text{-}K^2$ is observed for $LaTe_{1.40}$ at 1000°C.

## IV. DISCUSSION

Electron mobilities for $LaTe_y$ as a function of y can be calculated using carrier concentrations estimated from the y values

and the measured electrical resistivities. The carrier concentration n for $LaTe_y$ can be computed from Eq. 1, using a = 9.623 x $10^{-8}$ cm (Figure 1).

Mobilities calculated from $\mu = 1/ne\rho$ are presented in Figure 6. The solid symbols correspond to the samples whose properties are shown in Figures 2-5, and the open symbols represent duplicate samples or duplicate measurements. The mobilities decrease with temperature and also fall off sharply between y = 1.46 and y = 1.48. The room temperature mobilities are approximately double those reported for $LaS_y$.[3,4] The higher mobilities of $LaTe_{1.40}$ may contribute to the high power factors of $LaTe_{1.40}$. For a temperature range of 650-1000°C a $\ln\mu$ vs. lnT plot is linear (Figure 7). The slope of these lines versus y is shown in Figure 8. These slopes change with increasing y-values (increasing numbers of vacancies), possibly indicating a change in the predominant scattering mechanism. For $1.33 \leq y \leq 1.40$, the slope is approximately -1, indicating degenerate itinerant election conduction and acoustic scattering of carriers.

When $y \geq 1.44$, the magnitude of the slope is greater than 1. Since the number of lanthanum vacancies in the $LaTe_y$ structure increases with increasing y, the increased slope may result from an additional scattering mechanism associated with those vacancies.

However, in $LaS_y$, $\rho$ was found to be proportional to T up to 1000°C for values of y that spanned virtually the entire range $1.33 \leq y \leq 1.50$[3].

The Seebeck coefficient data for $LaTe_y$ can be analyzed to yield Fermi levels, reduced Fermi energies, and density-of-states effective masses. For itinerant electron or hole conduction described by solutions to the Boltzmann equation that are linear in energy, and for parabolic energy bands, one can write [6]

$$S = \pm (k/e) \left[ \left[ \frac{p+2}{p+1} \right] \left[ \frac{F_{p+1}(\eta)}{F_p(\eta)} \right] - \eta \right] \qquad \text{Eq. 2}$$

where the positive (negative) sign is for holes (electrons), and p describes the energy dependence of the carrier mean free path through $l=l_0E^p$. The Fermi integral $F_p(\eta)$ is defined by

$$F_p(\eta) = \int_0^\infty \epsilon^p f_0(\epsilon,\eta)\, d\epsilon,$$

where the equilibrium Fermi distribution is

$$f_0(\epsilon,\eta) = [1 + \exp(\epsilon-\eta)]^{-1},$$

and $\epsilon = (E-E_C)/kT$ and $\eta = (\phi-E_C)/kT$; $E_C$ = energy of conduction band minimum, and $\phi$ = chemical potential for electrons. The tabulated Fermi integrals [7] were fit by ninth order polynomials in $\eta$, making Equation 2 a polynomial equation. For each measured value of S, the value of $\eta$ that satisfied the polynomial version of Equation 2 was computed, using MathCAD routines, and assuming acoustic lattice scattering (p=0).

The reduced Fermi energies ($\eta$) and the Fermi levels ($\eta$kT) for $LaTe_y$ as functions of temperature are shown in Figures 9 and 10. The degree of degeneracy decreases as y increases from 1.33 to 1.48, consistent with the decrease in carrier densities as y increases.

The density-of-states effective mass m* for a parabolic band can be computed from the Fermi energies, using [7]

$$n = \frac{4}{\sqrt{\pi}} \left[ \frac{2\pi m^* kT}{h^2} \right]^{3/2} F_{1/2}(\eta), \qquad \text{Eq. 3}$$

where the carrier concentration n is computed from the value of y for each sample. Effective masses as a function of temperature are shown in Figure 11. The effective masses computed for $LaTe_{1.33}$ - $LaTe_{1.44}$ are only weakly dependent on temperature, and have values similar to those reported for $LaS_y$ ($1.33 < y < 1.50$).[3] The computed effective masses for $LaTe_{1.46}$ and $LaTe_{1.48}$, on the other hand, increase sharply

with increasing temperature. $LaTe_{1.44}$ appears to have a slight increase in effective mass with temperature. This indicates that for each value of T, the computation yields some kind of average value over all conduction electrons rather than a single temperature-dependent number that characterizes all electrons. Possibly some electrons move in a heavy-mass band that is not far removed in energy from the main conduction band.

The apparent increase in m* at high temperature and for $y \geq 1.44$ is consistent with the decrease in electron mobility noted above in connection with Figures 7 and 8. As noted above, the decrease in mobility below $\mu \alpha T^{-1}$ that we observe for $LaTe_y$ ($y \geq 1.44$) was not observed in $LaS_y$. Similarly, when we compute m* from the Seebeck coefficient of $LaS_{1.48}$ (data from Ref. 3), we find no significant dependence of m* on temperature.

## IV. CONCLUSIONS

Thermoelectric properties of $LaTe_y$, $1.33 \leq y \leq 1.48$ have been completed on single phase hot pressed specimens. This work is significant because previous investigations either included only a small portion of the solid solution region or the specimens contained appreciable amounts (i.e. identifiable by x-ray diffraction) of an oxygen-containing phase. We have found the thermoelectric properties

vary smoothly over the solid solution region, with the electrical resistivities and Seebeck coefficients increasing with y. In addition, for $y \geq 1.46$, the effective mass increases with temperature, in contrast to $LaS_y$ with the same structure, where no such effect is observed. The potential of $LaTe_y$ as a useful high temperature thermoelectric material depends on its figure-of-merit; measurements are currently underway to measure thermal conductivities so figures-of-merit can be computed.

## ACKNOWLEDGEMENT

The work described in this paper was performed for the Jet Propulsion Laboratory, California Institute of Technology, under contract with the National Aeronautics and Space Administration.

## REFERENCES

1. L.R. Danielson, V. Raag, and C. Wood, Proc. IECEC, Miami Beach, Florida, 1985, p. 3.531.

2. M. Cutler, J.F. Leavy, and R.L. Fitzpatrick, Phys. Rev. 133 (1964) A1143; J. Phys. Chem. Solids, 24 (1963) 319.

3. C. Wood, A. Lockwood, J. Parker, A. Zoltan, D. Zoltan, L.R. Danielson, and V. Raag, J. Appl. Phys. 58 (1985) 1542.

4. T. Takeshita, K.A. Gschneider, Jr., & B.J. Beaudry, J. Appl. Phys. 57 (1985) 4633.

5. L.R. Danielson, S. Matsuda, and V. Raag, Proc. 19th IECEC, 1984, Vol. 4, 2256.

6. A.F. Ioffe, Semiconductor Thermoelements and Thermoelectric Cooling, Infosearch Limited, London, 1957.

7. J.S. Blakemore, Semiconductor Statistics, Pergamon Press, 1962.

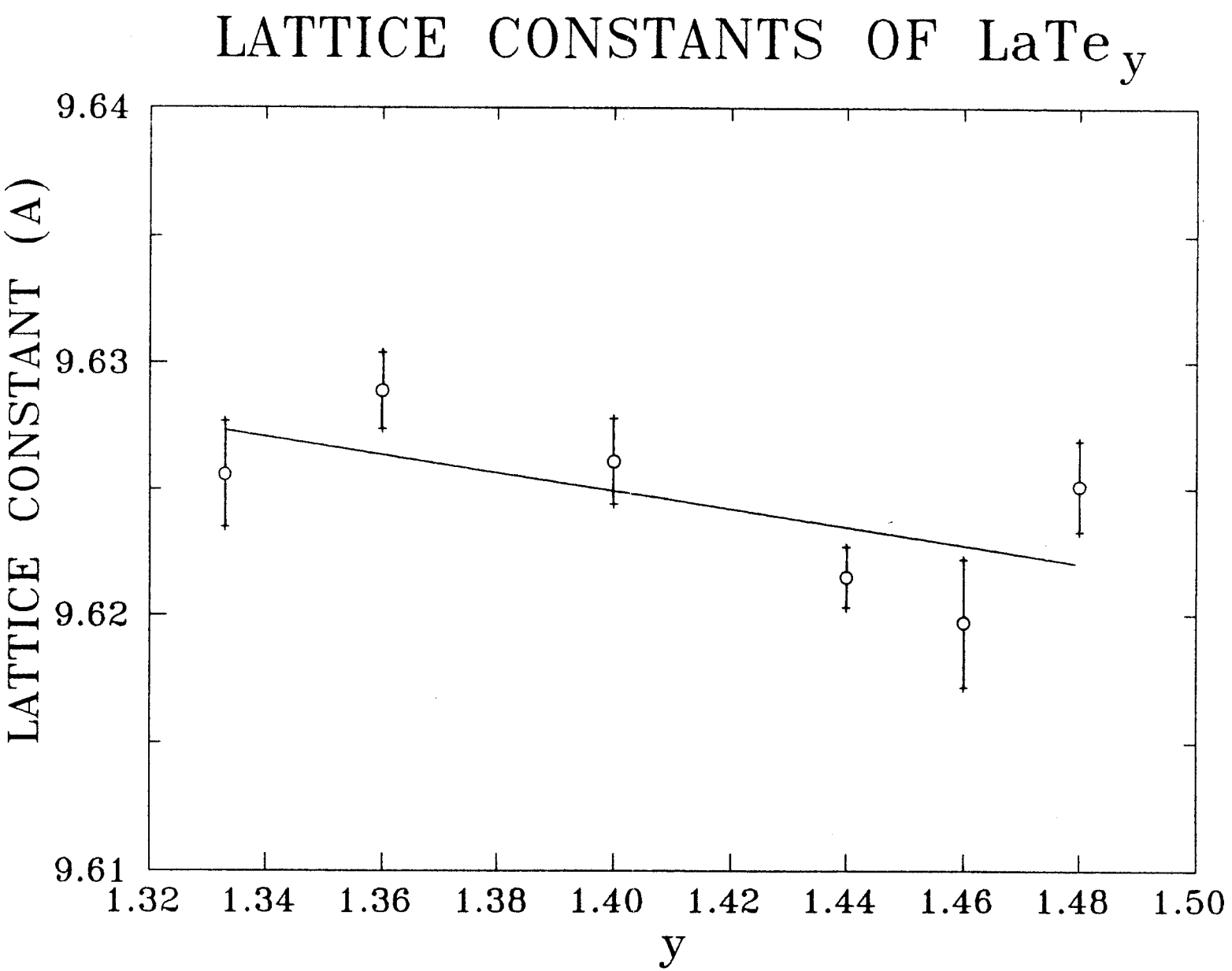
LATTICE CONSTANTS OF LaTe$_y$
LATTICE CONSTANT (A)
9.64
9.63
9.62
9.61
1.32
1.34
1.36
1.38
1.40
1.42
1.44
1.46
1.48
1.50
y

Fig. 1

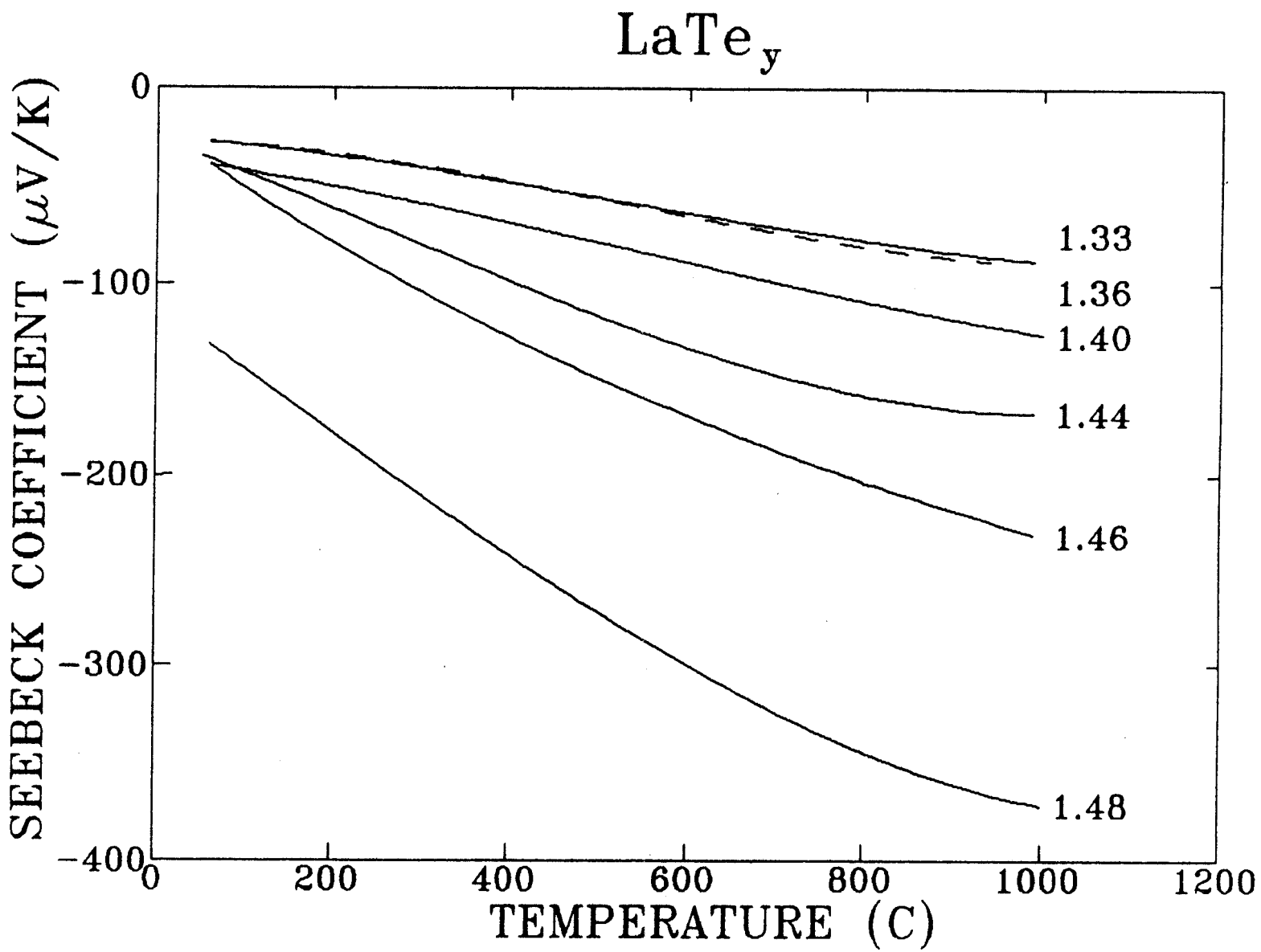
LaTe$_y$
SEEBECK COEFFICIENT ($\mu$V/K)
0
-100
-200
-300
-400
0
200
400
600
800
1000
1200
TEMPERATURE (C)
1.33
1.36
1.40
1.44
1.46
1.48

FIGURE 2

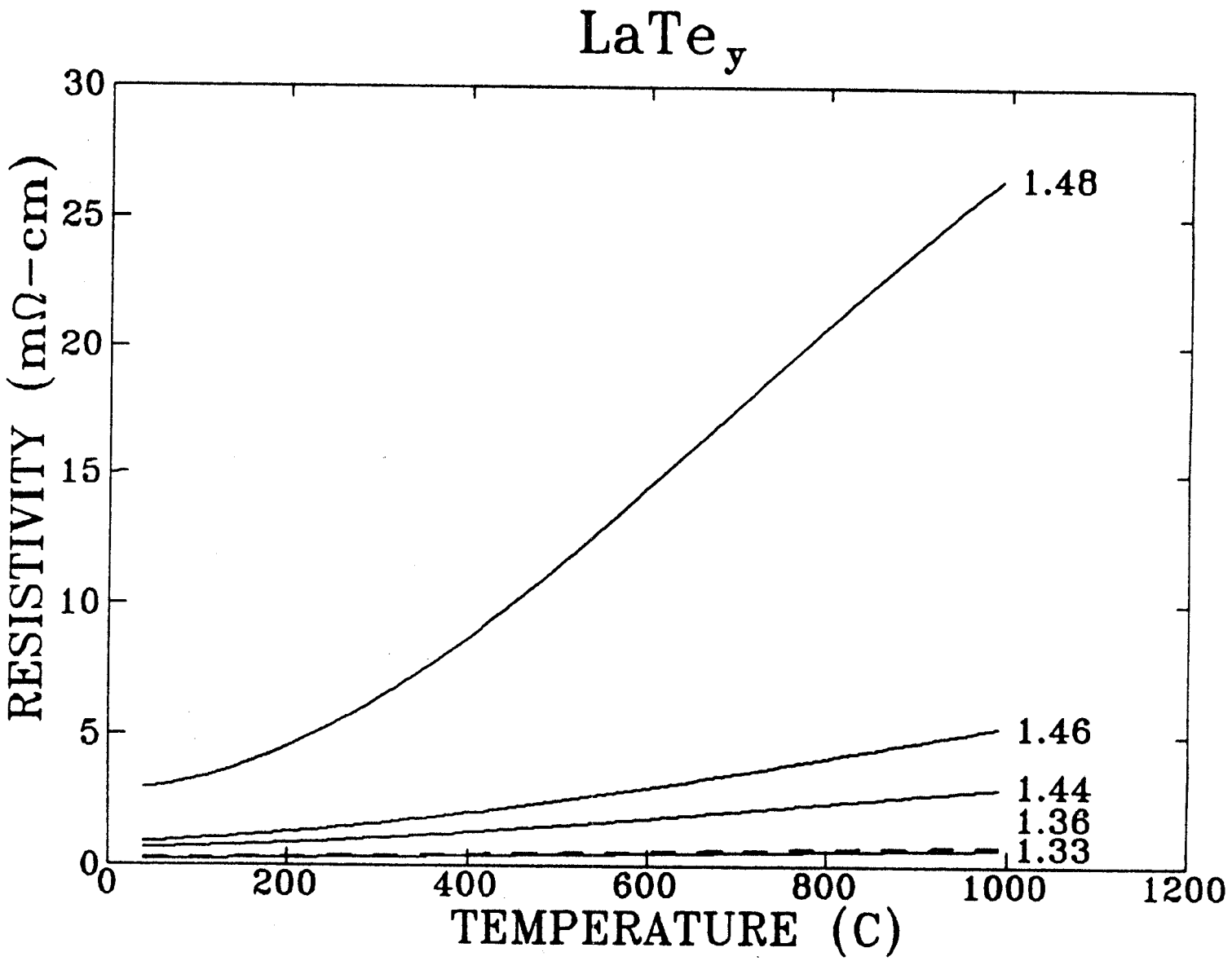
LaTe$_y$
RESISTIVITY (mΩ-cm)
30
25
20
15
10
5
0
0
200
400
600
800
1000
1200
TEMPERATURE (C)
1.48
1.46
1.44
1.36
1.33

FIGURE 3

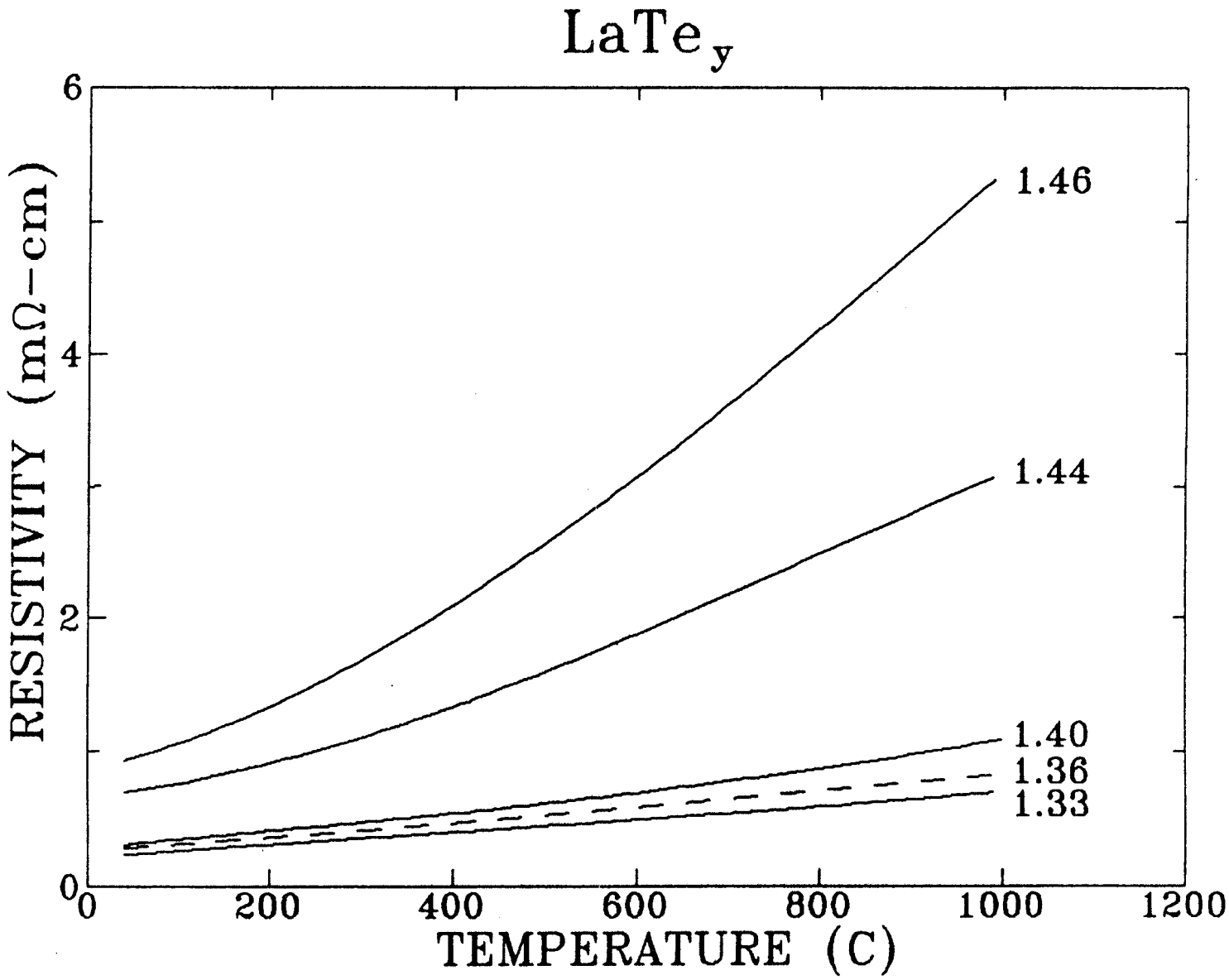
LaTe$_y$
RESISTIVITY (mΩ-cm)
TEMPERATURE (C)
0
2
4
6
0
200
400
600
800
1000
1200
1.46
1.44
1.40
1.36
1.33

FIGURE 4

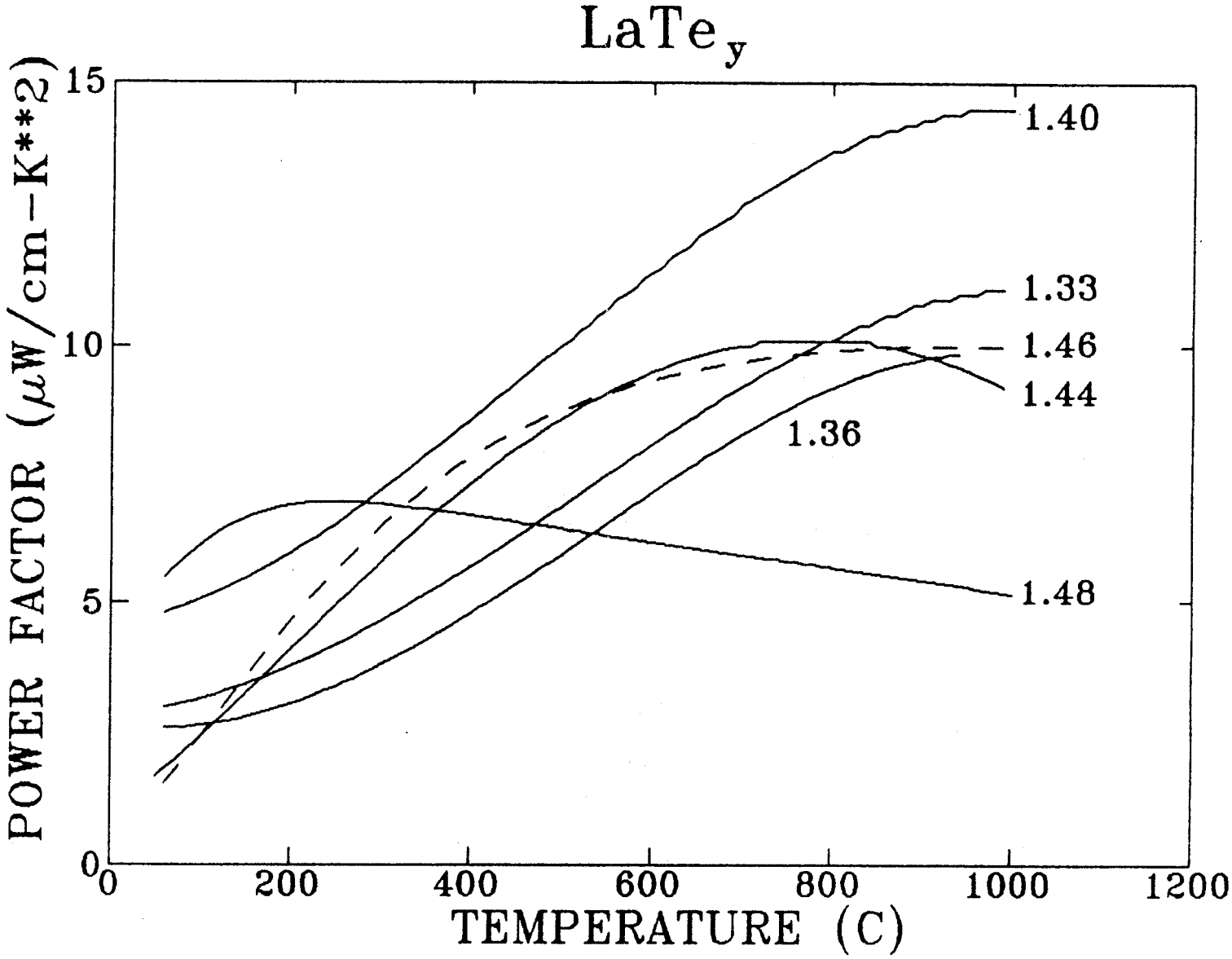
LaTe y
POWER FACTOR (μW/cm-K**2)
15
10
5
0
0
200
400
600
800
1000
1200
TEMPERATURE (C)
1.40
1.33
1.46
1.44
1.36
1.48

FIGURE 5

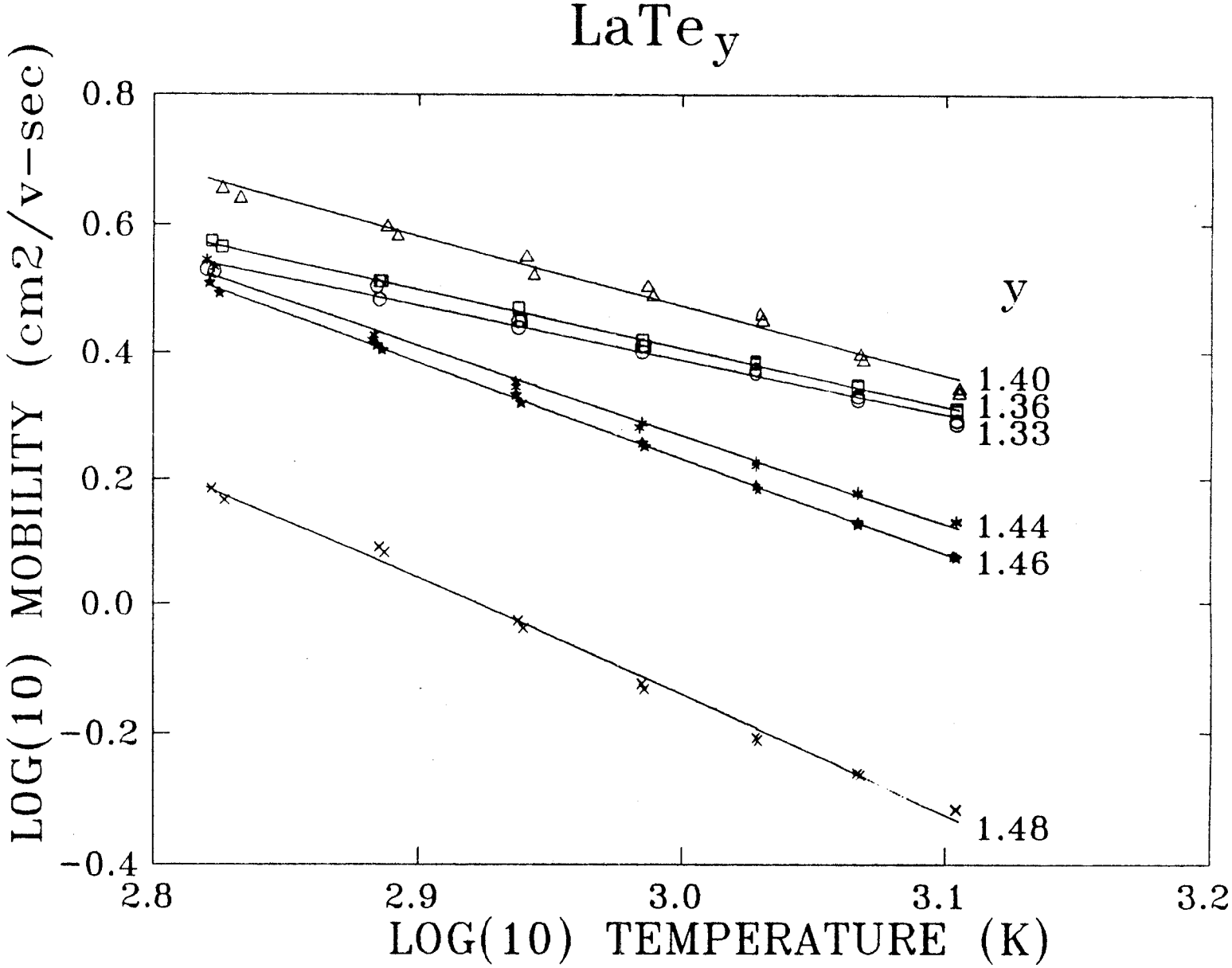
LaTe y
LOG(10) MOBILITY (cm2/v-sec)
0.8
0.6
0.4
0.2
0.0
−0.2
−0.4
2.8
2.9
3.0
3.1
3.2
LOG(10) TEMPERATURE (K)
y
1.40
1.36
1.33
1.44
1.46
1.48

Fig. 7

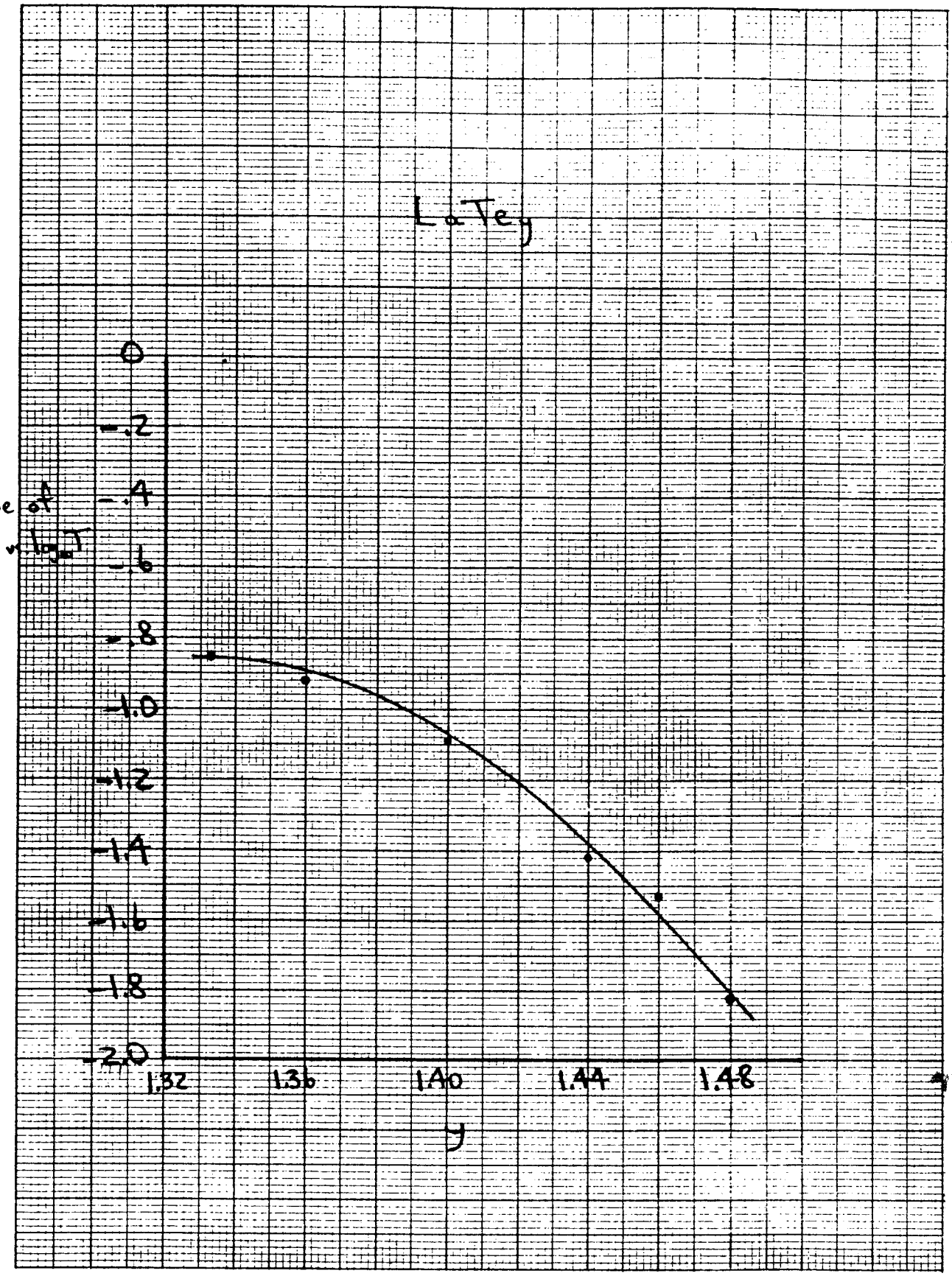

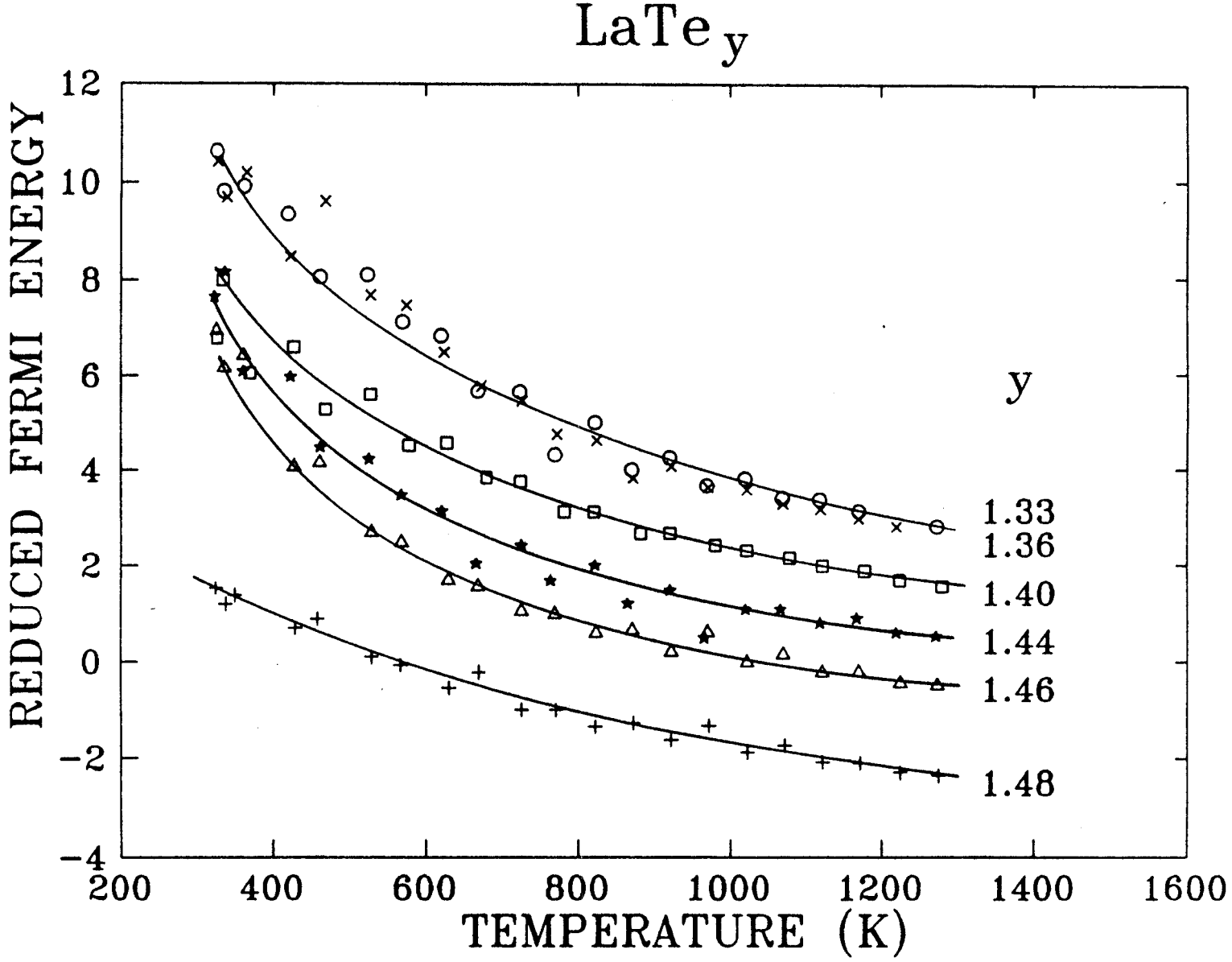
LaTe y
REDUCED FERMI ENERGY
TEMPERATURE (K)
y
1.33
1.36
1.40
1.44
1.46
1.48
12
10
8
6
4
2
0
−2
−4
200
400
600
800
1000
1200
1400
1600

Fig. 9

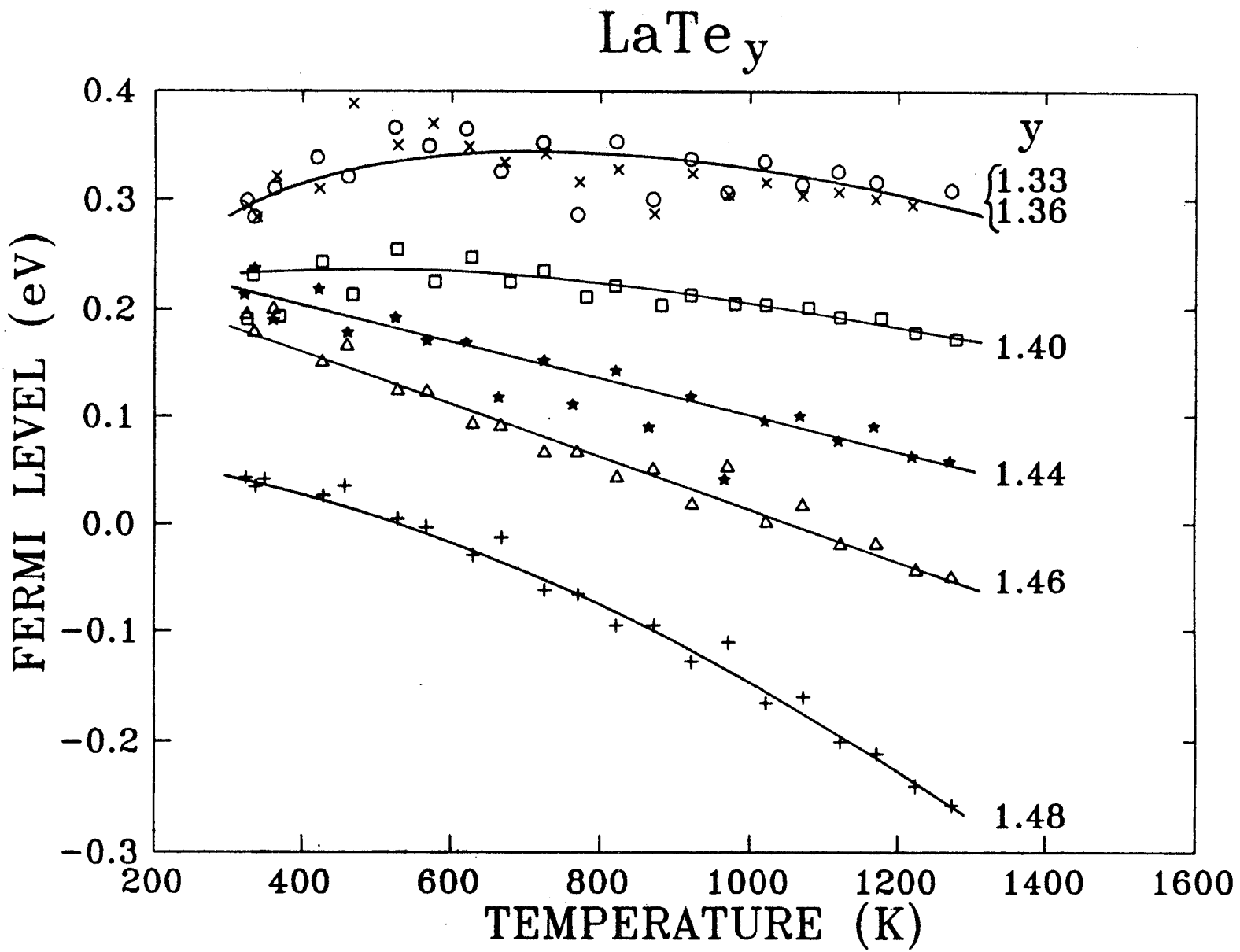
LaTe y
FERMI LEVEL (eV)
TEMPERATURE (K)
y
1.33
1.36
1.40
1.44
1.46
1.48
0.4
0.3
0.2
0.1
0.0
−0.1
−0.2
−0.3
200
400
600
800
1000
1200
1400
1600

Fig. 10

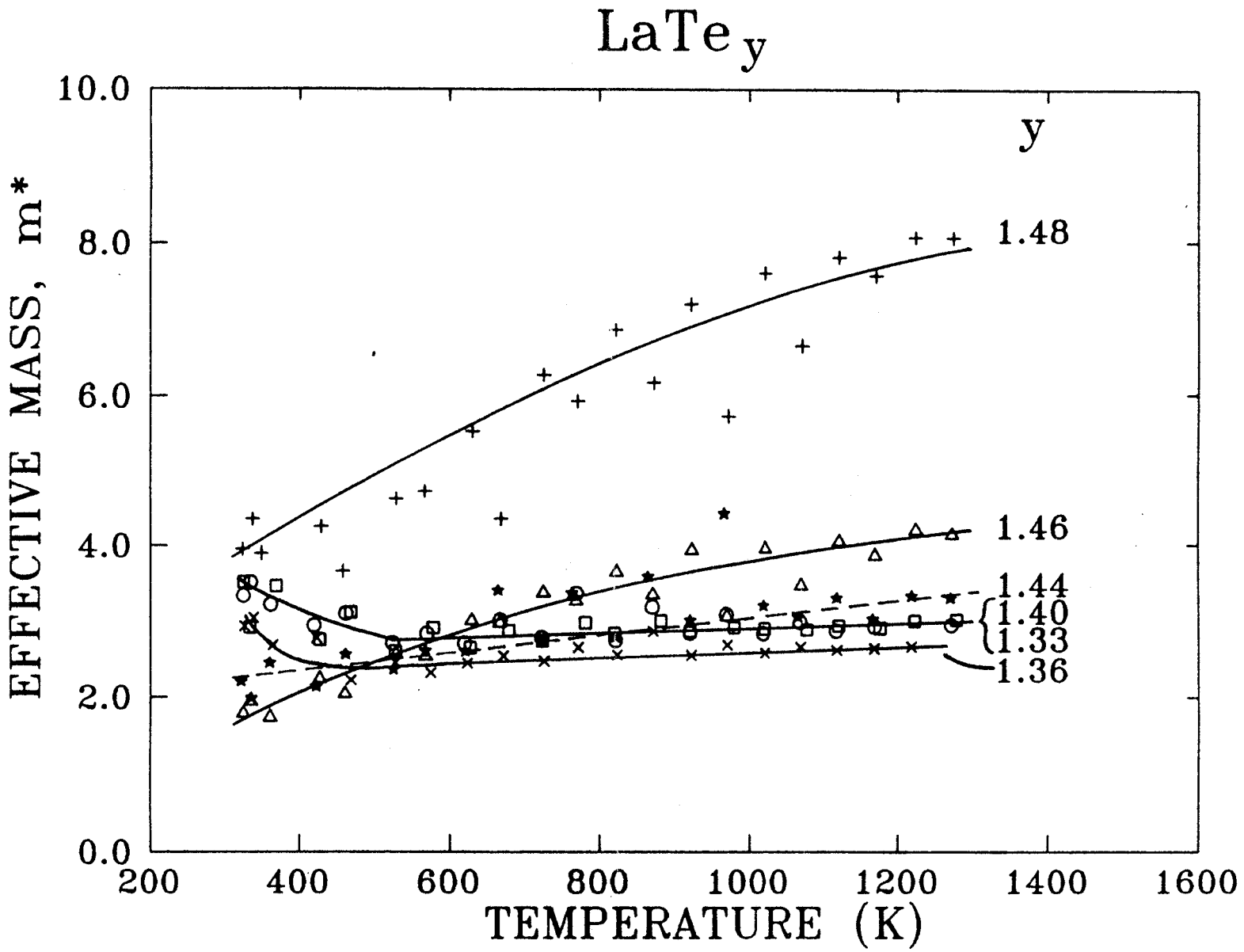
LaTe y
EFFECTIVE MASS, m*
TEMPERATURE (K)
y
1.48
1.46
1.44
1.40
1.33
1.36
10.0
8.0
6.0
4.0
2.0
0.0
200
400
600
800
1000
1200
1400
1600

Fig. 11